SIMULATION STUDIES OF DEPOSITION MECHANISMS FOR AEROSOL PARTICLES IN FIBROUS FILTERS INCLUDING SLIP FLOW

Andreas Wiegmann(*), K. Schmidt, S. Rief, L. Cheng and A. Latz
Fraunhofer Institut für Techno- und Wirtschaftsmathematik,
Fraunhofer Platz 1, 67663 Kaiserslautern, Germany

ABSTRACT

A geometric model for the 3 dimensional structure of nonwoven was developed. It contains the porosity, fiber diameters and fiber anisotropy as parameters, and results in large three-dimensional discretized realizations of the media. In these structures, the fluid flow and particle deposition are simulated. Initial pressure drop, filter efficiency and filter lifetime are quantities that are computed based on the nonwoven, the mean flow velocity and the particle size distribution. Here the focus is on isolating the effects of different deposition mechanisms, fiber diameter, solid volume fraction and flow regime on the filter efficiency and establishing qualitative agreement with analytic formulas as well as measurements.

KEYWORDS

Solid-Gas Separation, Simulation, Slip Flow, Nano Particles, Nano Filtration.

1. Introduction

It has been a long-standing question what the model for computing filtration efficiencies in [4] predicts regarding the individual filtration effects interception, inertial impaction and diffusion. The model seems to predict only the filtration efficiency for all effects at the same time. The purpose of this paper is to illustrate that it is possible to separate out the influence of the different effects and that the results agree with analytic formulas as well as measurements from [1]. This is needed to establish the validity of simulations so that they can then also be used for regimes where formulas do not apply or where experiments would be too costly.

2. Method

The whole thickness of the filter media needs to be discretized in order to retrieve directly filter efficiencies that are comparable with measurements. An inflow region helps avoiding artifacts in the fluid flow and allows particles to develop their own motion before entering the filter media. The computational domain is thus usually box-shaped, with the long side of the box taken across the filter media and the other two sides as long as the computer memory permits. This box is composed by $n_x \times n_y \times n_z$ cubic grid cells. Each of these cells can be solid or empty, meaning it is part of a fiber or part of the flow domain, respectively. Experience shows that to achieve resolution-independent results for the filter efficiency, fibers should be resolved with 10 or more voxels per diameter. This is about twice better resolution than what is needed for permeability computations. It is a serious constraint because this means 8 times more grid cells are needed for three-dimensional computations. At a typical resolution, 1.4 micron, a 1.4 mm thick filter media requires 1000 voxels, with additional 120 cells as inflow region. In the two cross directions about 300 cells can be used in order to still fit the flow computation in 16 GB of computer memory. Following [2], fibers are discretized by setting to solid all the cells within the fiber radius from the fiber axis. At 1.4 micron resolution, a 14 micron fiber is resolved with 10 cells per diameter. For such small regimes, the fibers may be assumed as straight. The desired solid volume fraction is achieved by randomly placing fibers and adding up their contribution. This is done by

counting the number of cells that are set to solid when placing the fiber. In typical media the fibers are oriented randomly yet preferably perpendicular to the flow. Stationary slow gas flows in the no-slip regime may be described by the Stokes equations with periodic boundary conditions:

$$\begin{aligned} -\mu\Delta\vec{u} + \nabla p &= 0 \text{ (momentum balance)} \\ \nabla \cdot \vec{u} &= 0 \text{ (mass conservation)} \\ \vec{u} &= 0 \text{ on } \Gamma \text{ (no-slip on fiber surfaces)} \\ P_{in} &= P_{out} + c \text{ (pressure drop is given)} \end{aligned}$$

Here μ is the fluid viscosity, $\vec{u}$ is the (periodic) velocity and p is the pressure (periodic up to the pressure drop in the flow direction). We use the finite difference approach on staggered grids [3, 6] and interpolate the computed velocities from the cell faces in order to have a continuous velocity field that is needed for particle tracking. Note that the above linear formulation allows simply rescaling the flow field to adjust it to a desired mean velocity. This rescaling is only possible in the considered regime of slow flows, or low Reynolds number flows. For smaller fiber diameters, it is well known [8] that no-slip boundary conditions are not appropriate, and instead slip boundary conditions are applied.

$$\begin{aligned} -\mu\Delta\vec{u} + \nabla p &= 0 \text{ (momentum balance)} \\ \nabla \cdot \vec{u} &= 0 \text{ (mass conservation)} \\ \vec{n} \cdot \vec{u} &= 0 \text{ on } \Gamma \text{ (no flow into fibers)} \\ \vec{t} \cdot \vec{u} &= -\lambda\nabla\left(\vec{u} \cdot \vec{t}\right) \cdot \vec{t} \text{ on } \Gamma \text{ (slip flow along fibers)} \\ P_{in} &= P_{out} + c \text{ (pressure drop is given)} \end{aligned}$$

Here $\vec{n}$ is the normal direction to the fiber surface, λ is the slip length and $\vec{t}$ is any tangential direction with $\vec{t} \cdot \vec{n} = 0$. For the same pressure drop, computed velocities for slip boundary conditions are higher than for no-slip boundary conditions. Conversely, for a given velocity or equivalently, a given mass flux, the pressure drop is lower when computed with slip boundary conditions. The challenge and restriction to our method lies in the need for the tangential directions to the surface: On cubic cells, only axis-parallel tangents can be resolved, and this limits our ability to compute correctly cases with larger slip length λ, [7]. To compute the filtration efficiency, particles are placed at random positions at the beginning of the inflow regime. These particles are then tracked according to increasingly complex laws of motion that are always based on the air flow. Assuming that the particle concentration is low enough, this air flow is not altered by the presence of the particles. If during this tracking procedure a particle touches a fiber surface, then in the *caught on first touch* model it is captured and accounted for as filtered. The percentage of captured particles is called the filtration efficiency. All results are based on this caught on first touch model. Three distinct effects that contribute to the filtration efficiency are commonly described in the literature [8]. First, simply by following a stream line of the flow, a particle may get so close to a fiber that it touches. This effect is called *interception*. Secondly, based on its mass a particle may leave a curving stream line and travel straight due to its inertia. This effect is called *inertial impaction*. Finally, very small particles may leave the trajectory based on the flow and inertia due to random hits by air molecules. This effect is called *Brownian diffusion*. To account for interception, the particle should travel with flow velocity $\vec{u}$,

$$d\vec{x} = \vec{u}(\vec{x}(t))dt.$$

Here $\vec{x}(t) = (x_1(t), x_2(2), x_3(t))$ is the position of the particle at time t. Recall from above that $\vec{u}$ was computed based on Stokes-flow with slip or no-slip boundary conditions. The introduction of friction with the fluid flow with friction coefficient γ adds the effect of inertial impaction, neglecting the feedback of the particles motion on the fluid flow. The friction model

is based on Stokian friction of spherical particles [4], now supplemented by the Cunningham Slip Correction Factor $C_c(Kn)$ as introduced in [9] for solid particles at NTP conditions. $Kn = \lambda / R$ is the Knudsen number defined as the ration between the mean free path λ and the radius *R* of the particle. We explicitly introduce the particles velocity as a separate variable $\vec{v}$ and write

$$
\begin{aligned}
d\vec{v} &= -\gamma \times \left(\vec{v}(\vec{x}(t)) - \vec{u}(\vec{x}(t))\right) dt, \\
d\vec{x} &= \vec{v}(\vec{x}(t)) dt, \\
\gamma &= 6\pi\rho\mu \frac{R}{C_c m}, \\
C_c &= 1 + Kn\left[1.142 + 0.558 e^{-0.999/Kn}\right].
\end{aligned}
$$

For fixed fluid density ρ and particle radius R the friction coefficient tends to infinity as the particle mass m tends to zero. In the limiting case $m = 0$ the previous equation is recovered, i.e. for $m = 0$ the particle velocity is simply the fluid velocity. Finally, interception, inertial impaction and Brownian motion of particles altogether are described in [4] by the stochastic ordinary differential equation

$$
\begin{aligned}
d\vec{v} &= -\gamma \times \left(\vec{v}(\vec{x}(t)) - \vec{u}(\vec{x}(t))\right) dt + \sigma \times d\vec{W}(t), \\
d\vec{x} &= \vec{v}(\vec{x}(t)) dt, \\
\sigma^2 &= \frac{2 k_B T \gamma}{m}, \\
\langle dW_i(t), dW_j(t) \rangle &= \delta_{ij} dt.
\end{aligned}
$$

Here T is the ambient temperature, k_B is the Boltzmann constant and $d\vec{W}(t)$ is a 3d probability (Wiener) measure.

3. Results

The initial positions of spherical particles are drawn from an equidistribution of particles of 0.01 µm, 0.02 µm, 0.05 µm, 0.1 µm, 0.2 µm, 0.5 µm, 1 µm, 2 µm, 5 µm and 10 µm. 10000 particles are considered for each of the 10 particle sizes. This particle size distribution is not physical but chosen to make sure that enough particles of all sizes are used in order to get correct statistics. Figure 1 (right) shows 10000 deposited particles in the middle structure shown in Figure 1 (left). Only the largest ones are visible as blue spheres on the fibers. For each of the 5 filter media in Figure 1 (left), Stokes Flow with no-slip boundary conditions was pre-computed. For the middle structure, also slip-boundary conditions were considered. The computed pressure drop at $U = 1 m/s$ was 247, 138, 85 (78 for slip boundary conditions), 60 and 46 Pa, respectively. So, the improvement in filter efficiency observed below also correlates with increased energy requirements for the operation of the filter.

Figure 2 (left) shows the individual contributions to the filter efficiency of the interception, impaction and diffusion mechanisms by predicted our simulations, on the right we show the analytic formula based predictions from [1].

We observe qualitatively the same contribution of individual filtration effects (Figure 2 left), the same shift in most penetrating particle size for higher flow velocities (Figure 3 left), lower filter efficiency of thicker fibers (Figure 3 right), higher filter efficiency for higher solid volume fraction (Figure 4 left), and in addition a small decrease in filter efficiency due to slip flow (Figure 4 right). The trends in Figure 2 as well as Figures 3 and 4 agree well with the analytical and experimental results from [1]. Due to differences in the regime of fiber diameter d_F , velocity U , solid volume fraction α and media thickness L lower filter efficiencies than in [1] would be expected, but higher ones are observed. Two model parameters that are currently investigated to close this gap are the resolution and modifications to the caught on touch model that allow particles to detach from fibers.

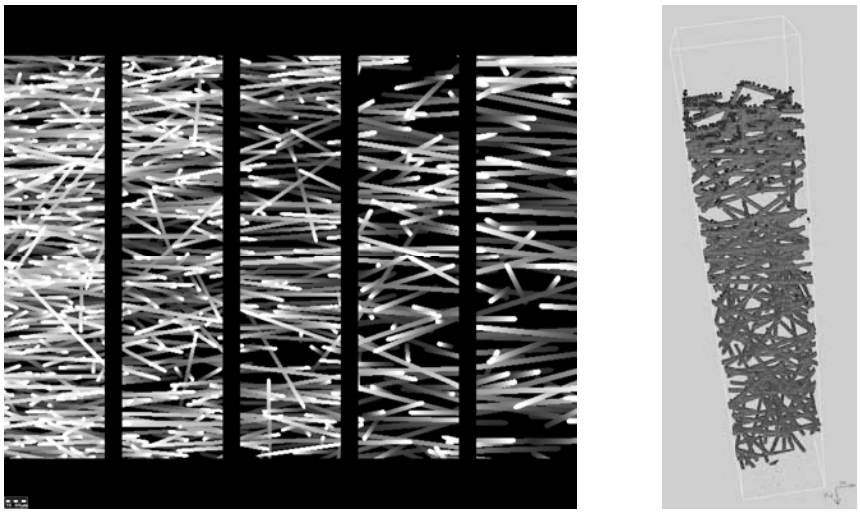

Figure 1: Left: Simulated REM view of the 5 structures. From left to right ($\alpha = 0.1$ $d_F = 14\mu m$), ($\alpha = 0.07$ $d_F = 14\mu m$), ($\alpha = 0.05$ $d_F = 14\mu m$), ($\alpha = 0.05$ $d_F = 17\mu m$), ($\alpha = 0.05$ $d_F = 20\mu m$). Right: 3d visualization of structure and deposited particles.

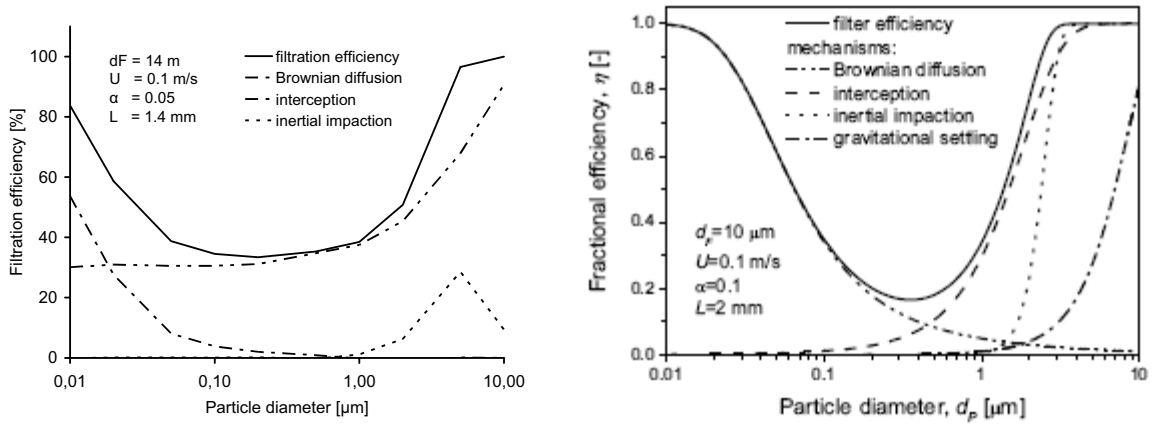

Figure 2: Influence of filtration effects on filter efficiency. Left: Simulation, right: analytic [1].

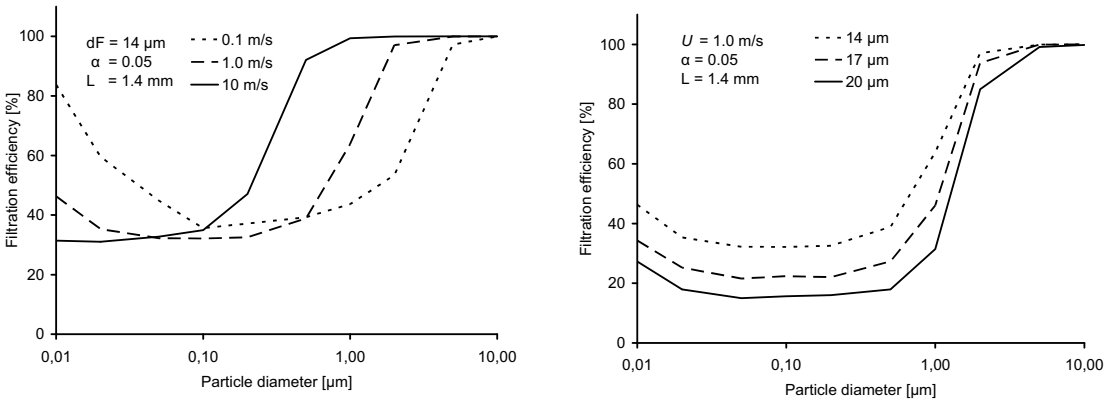

Figure 3: Influence of velocity and fiber diameter on filter efficiency.

4. Conclusions

Simulations can quantify the contributions of a variety of individual filtration effects and the results agree quantitatively with the analytical and experimental results in [1]. The strength of the simulations is two-fold: first, they are able to predict the pressure drop of the filter media, which is not available in [1]. Secondly, simulations apply also where analytic formulas are not yet available, in cases of fiber diameter distributions or graded media, for example. In these cases, simulations can be of great value for the purposes of optimizing fibrous filter media.

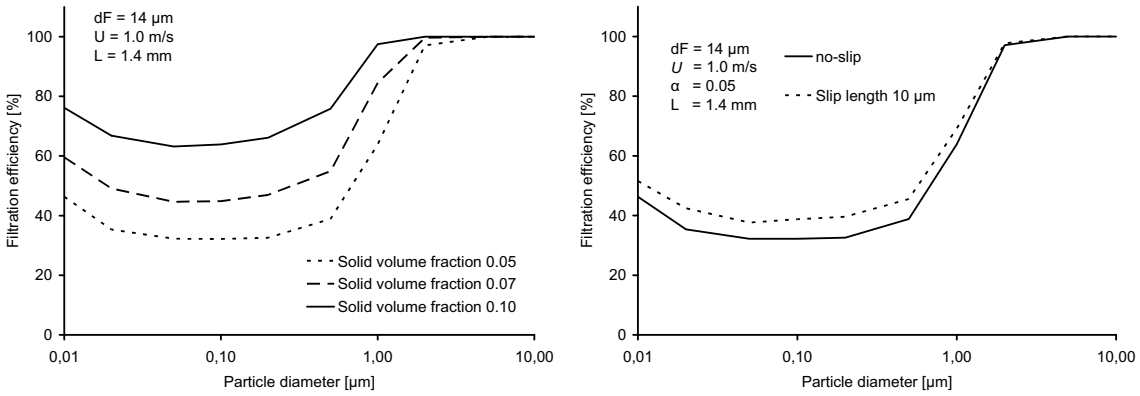

Figure 4: Influence of solid volume fraction and slip boundary conditions on filter efficiency.

References

[1] A. Balazy and A. Podgorski, *Theoretical and experimental study on the most penetrating particle size of aerosol particles in fibrous filters*. Filtech 2007, Volume II, pp. II-192 - II-199, February 2007.

[2] K. Schladitz, S. Peters, D. Reinel-Bitzer, A. Wiegmann, J. Ohser, *Design of acoustic trim based on geometric modeling and flow simulation for nonwoven*, Computational Material Science, Vol. 38. No 1, 2006.

[3] A. Wiegmann, *Computation of the permeability of porous materials from their microstructure by FFF-Stokes*, Berichte des Fraunhofer ITWM, Nr. 129, 2007.

[4] A. Latz and A. Wiegmann, *Simulation of fluid particle separation in realistic three dimensional fiber structures*, Filtech Europa, Vol 1, pp. I-353-I-361, October 2003.

[5] S. Rief, A. Latz and A. Wiegmann, *Research Note: Computer simulation of Air Filtration including electric surface charges in three-dimensional fibrous micro structures*, Filtration, Vol. 6, No. 2, 2006.

[6] L. Cheng and A. Wiegmann, *EJ-Stokes: an explicit jump correction to FFF-Stokes*, in preparation, 2008.

[7] L. Cheng and A. Wiegmann, *EJ-Stokes solver with slip boundary conditions*, in preparation, 2008.

[8] R.C. Brown, *Air Filtration, an Integrated Approach to the Theory and Application of Fibrous Filters*, Pergamon Press, Oxford (1993).

[9] M.D. Allen, and O.G. Raabe, *Slip correction measurements of spherical solid aerosol-particles in an improved Milikan apparatus,* Aerosol Sci. Technol. 4(3):269-286, 1985.